

## Precise and Convenient Size Barcode Method on Microfluidic Chip for Multiplex Biomarkers Detection

*Man Tang<sup>a, b, c</sup>, Jinyao Chen<sup>a</sup>, Jia Lei<sup>a</sup>, Zhao Ai<sup>a, b, c</sup>, Feng Liu<sup>a, b, c</sup>, Shao-Li Hong<sup>\*a, b, c</sup>, and Kan Liu<sup>\*a, b, c</sup>*

<sup>a</sup> School of Electronic and Electrical Engineering, Wuhan Textile University, Wuhan 430200, People's Republic of China.

<sup>b</sup> Hubei Engineering and Technology Research Center for Functional Fiber Fabrication and Testing, Wuhan Textile University, Wuhan 430200, People's Republic of China.

<sup>c</sup> Hubei Province Engineering Research Center for Intelligent Micro-nano Medical Equipment and Key Technologies, Wuhan 30200, People's Republic of China

\* Co-corresponding e-mail: [slhong@whu.edu.cn](mailto:slhong@whu.edu.cn); (S. -L. Hong); liukan2002@gmail.com (K. Liu);

### S.1. Characterization of the wedge-shaped microfluidic chip

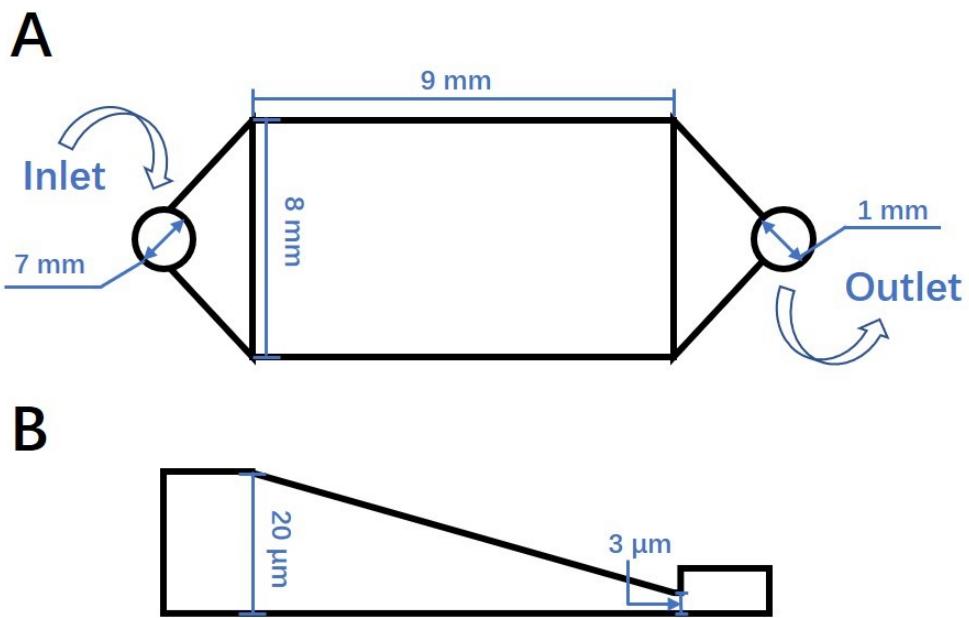


**Figure S1.** Schematic diagram of the wedge-shaped microfluidic chip for multiplex biomarker detection, with detailed structural parameters labelled. (A) Top view of the microfluidic chip. (B): Lateral view of the microfluidic chip, with detailed structural parameters labelled.

## S.2. Characterization of the traditional step microfluidic chip

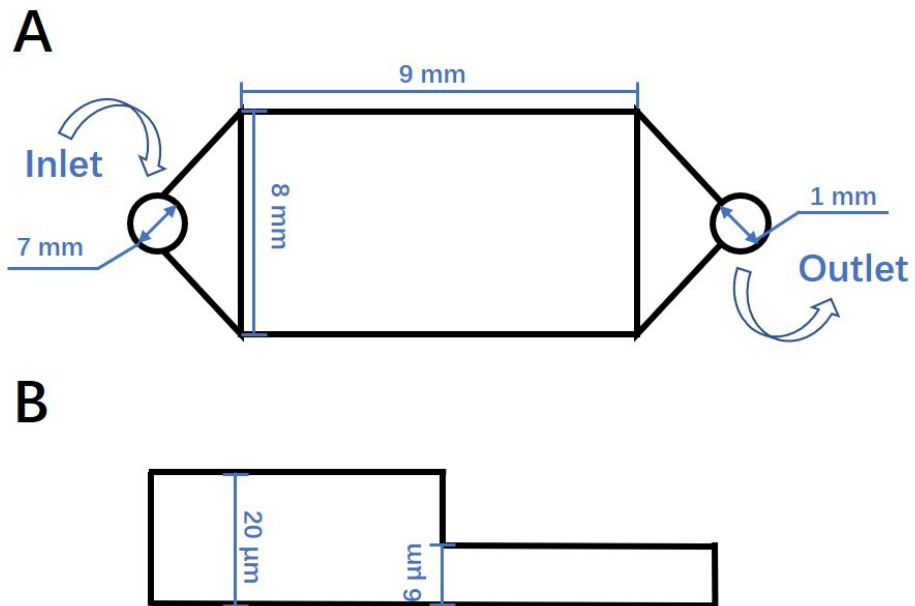


**Figure S2.** Schematic diagram of the traditional step microfluidic chip, with detailed structural parameters labelled. (A) Top view of the microfluidic chip. (B): Lateral view of the microfluidic chip, with detailed structural parameters labelled.

### S.3. The influence of the introduced microparticles number on accuracy.

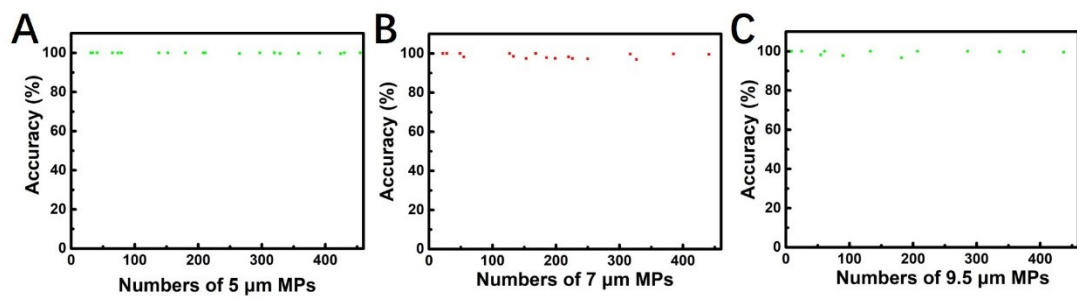


**Figure S3.** (A) The relationship between the number of 5  $\mu$ m fluorescent microparticles of green fluorescence introduced in the wedge-shaped microfluidic chip and the accuracy of the formed stripe. (B) The relationship between the number of 7  $\mu$ m fluorescent microparticles of red fluorescence introduced in the wedge-shaped microfluidic chip and the accuracy of the formed stripe. (C) The relationship between the number of 9.5  $\mu$ m fluorescent microparticles of green fluorescence introduced in the wedge-shaped microfluidic chip and the accuracy of the formed stripe.

#### S.4. The influence of the introduced microparticles concentration on accuracy.

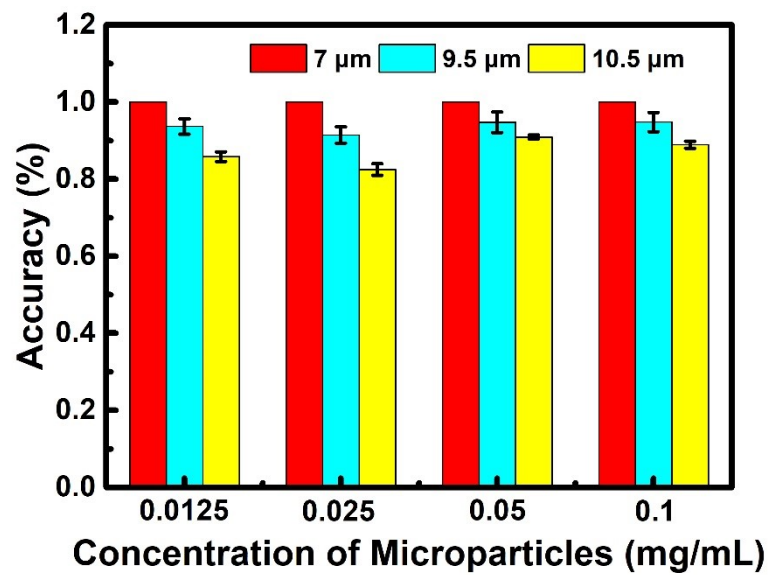


**Figure S4.** The relationship between the concentration of the mixed fluorescent microparticles (7  $\mu\text{m}$ , 9.5  $\mu\text{m}$ , and 10.5  $\mu\text{m}$ ) introduced in the wedge-shaped microfluidic chip and the accuracy of the formed stripes. Error bars represent the standard deviation of triplicate experiments.

### S.5. Capacity of the barcode for multiplex biomarker detection

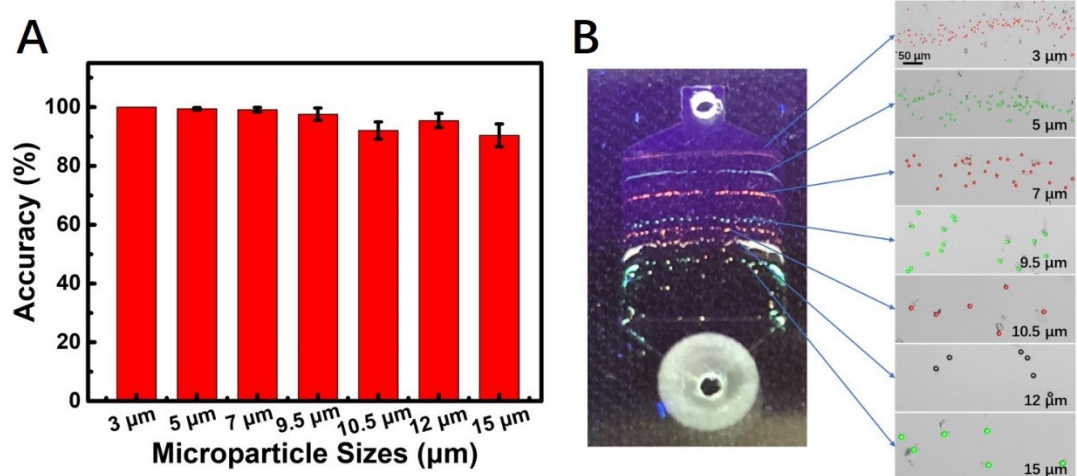


**Figure S5** (A) Accuracy of each stripe formed by 3  $\mu\text{m}$ , 5  $\mu\text{m}$ , 7  $\mu\text{m}$ , 9.5  $\mu\text{m}$ , 10.5  $\mu\text{m}$ , 12  $\mu\text{m}$  and 15  $\mu\text{m}$  fluorescent microparticles. Error bars represent the standard deviation of triplicate experiments. (B) Photograph of the wedge-shaped microfluidic chip after capture 3  $\mu\text{m}$ , 5  $\mu\text{m}$ , 7  $\mu\text{m}$ , 9.5  $\mu\text{m}$ , 10.5  $\mu\text{m}$ , 12  $\mu\text{m}$  and 15  $\mu\text{m}$  fluorescent microparticles. The insert photographs were shown the fluorescent microparticles of 3  $\mu\text{m}$ , 5  $\mu\text{m}$ , 7  $\mu\text{m}$ , 9.5  $\mu\text{m}$ , 10.5  $\mu\text{m}$ , 12  $\mu\text{m}$  and 15  $\mu\text{m}$  under a fluorescent microscope, respectively.

### S.6. Loading capacity of wedge-shaped microfluidic chip

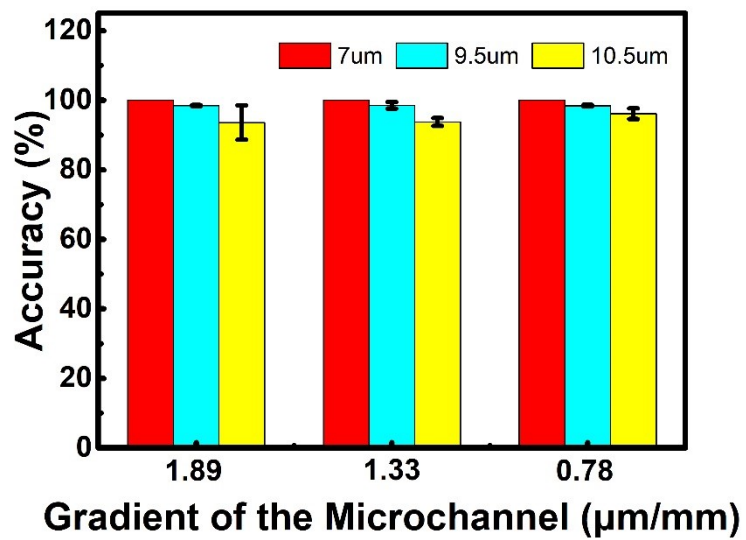


**Figure S6.** Accuracy of each stripe formed in the wedge-shaped microfluidic chip with gradient of 1.89  $\mu\text{m}/\text{mm}$ , 1.33  $\mu\text{m}/\text{mm}$ , and 0.78  $\mu\text{m}/\text{mm}$ , respectively. The numbers of the fluorescent microparticles of 7  $\mu\text{m}$ , 9.5  $\mu\text{m}$ , and 10.5  $\mu\text{m}$  in each experiment is about 250-300. Error bars represent the standard deviation of triplicate experiments.

### S.7. The proof-of-concept for the multiplex biomarker detection

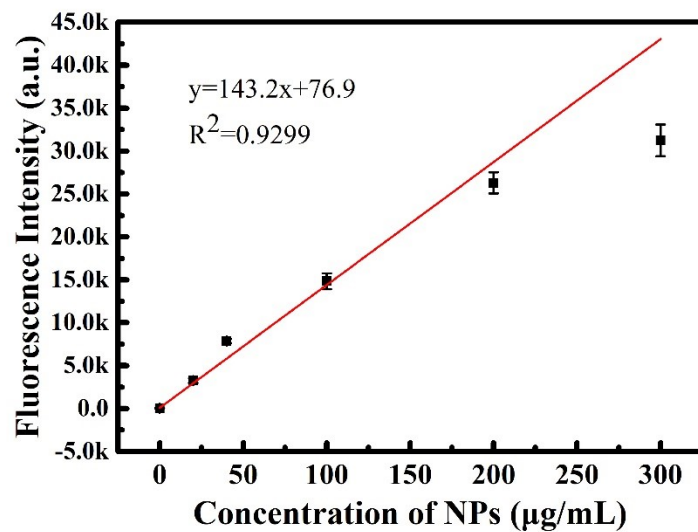


**Figure S7.** Linear relationship of fluorescence intensity *versus* NPs concentration from 0 to 300  $\mu\text{g}/\text{mL}$ . The linear relationship was obtained in a range of 20-300  $\mu\text{g}/\text{mL}$ , with a linear correlation coefficient ( $R^2$ ) of 0.9299.

### S.8. Analytical performance with microparticle of different sizes

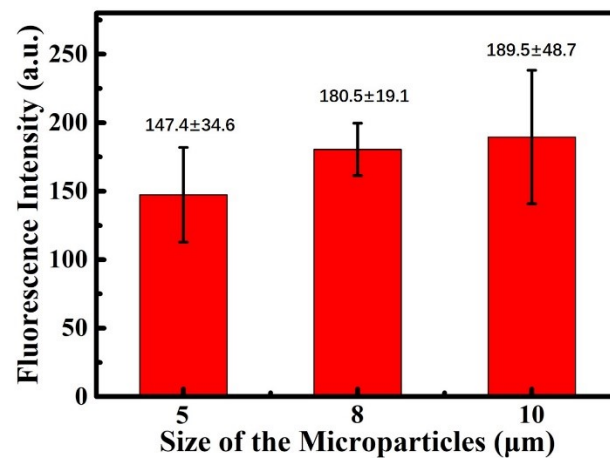


**Figure S8.** Fluorescence intensity of the microparticles (divided by their surface area) of different sizes (5, 8, and 10 microns) after incubating with 5  $\mu\text{g}$  IFNs. As it showed, the fluorescence intensity of the microparticles of different sizes had no significant difference except a slightly increase. This result might cause by the fluorescent images were obtained in two-dimensions, hence some deviations generated between the collected fluorescent signals and the actual fluorescence intensity on the microparticles.

### S.9. Multiplex biomarker detection of three kinds of DNAs

For the verification of the multiplex biomarker detection, we had designed three kinds of DNA. Thereinto, DNA1 was labelled by Alexa 488 with green fluorescence (emission 488 nm, excitation 519 nm), DNA 2 was labelled by Cy3 with red fluorescence (emission 570 nm, excitation 650 nm), and DNA 3 was labelled by Alexa Fluor 405 with blue fluorescence (emission 405nm, excitation 421 nm). The three kinds of DNA simultaneous detection were processed by the DNA hybridization. Firstly, microparticles (5  $\mu\text{m}$ , 8  $\mu\text{m}$ , and 10  $\mu\text{m}$ ) were coated with the capture-DNAs accordingly, and then about 0.2  $\mu\text{mol/L}$  of target DNAs were added simultaneously to hybridize. In this part, DNA1 was detected by 5  $\mu\text{m}$  microparticles, DNA2 was detected by 8  $\mu\text{m}$  microparticles, and DNA3 was detected by 10  $\mu\text{m}$  microparticles, respectively. As it shown in the **Figure S8**, the surface of each size of microparticles had a corresponding fluorescence signal, exhibiting the DNAs could be detected successfully. This experiment showed the performance of our proposed method in the multiplex detection.

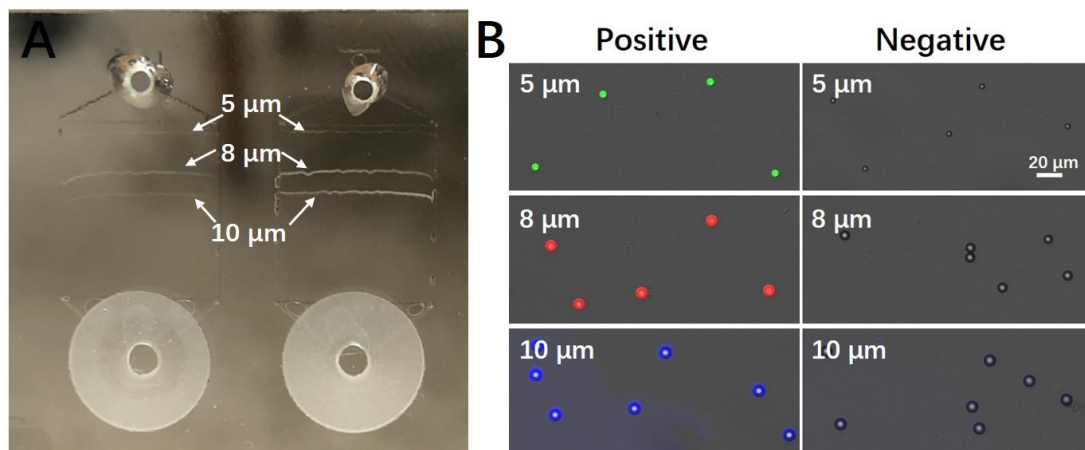


**Figure S9.** (A) Photographs of the wedge-shaped microfluidic chip with three kinds of DNA detection. The left one is positive experiments and the other one is negative experiments. (B) Fluorescence pictures taken by a fluorescent microscope of three kinds of DNA detection with 5  $\mu\text{m}$ , 8  $\mu\text{m}$ , and 10  $\mu\text{m}$  microparticles through the wedge-shaped microfluidic chip.